Morphological and physicochemical changes in the cassava (*Manihot esculenta*) and sweet potato (*Ipomoea batata*) starch modified by pyrodextrinization

Zeniff REYES-LÓPEZ[1], David BETANCUR-ANCONA[2], Jorge Luis BLE-CASTILLO[1], Isela Esther JUÁREZ-ROJOP[1],
Angela ÁVILA-FERNÁNDEZ[1], Maloy HERNÁNDEZ-HERNÁNDEZ[1], Carlos GARCÍA-VAZQUEZ[1],
Valentino Mukthar SANDOVAL-PERAZA[3], Patricia QUINTANA-OWEN[4], Viridiana OLVERA-HERNÁNDEZ[1]* 🆔

Abstract

In recent years, resistant starch (RS) and slowly digestible starch (SDS) have been linked to the prevention of chronic noncommunicable diseases, such as obesity and its complications. Southern Mexico has an important role in the tuber crop production of *M. esculenta* and *I. batatas*, which contain considerable amounts of starch. The aim of this study was to evaluate the morphological and physicochemical changes of *M. esculenta* and I. *batatas* after pyrodextrinization, including the production of RS and SDS. The factors used in this study were the starch/acid ratio (2.2 HCl) (80:1 and 160:1 p/v); temperature (90 °C and 110 °C) and reaction time (1 and 3 h). The highest production of RS in *M. esculenta* was obtained with the highest starch/acid ratio and temperature, and the lowest reaction time. For pyrodextrins, loss of crystallinity and an increase in swelling power and water absorption capacity were observed. The highest production of RS in *I. batatas* was obtained with the highest starch/acid ratio and reaction time, and the lowest temperature. Crystallinity and enthalpy of gelatinization decreased in modified starches. The solubility, swelling power and water absorption capacity increased in both sources.

Keywords: functional properties; resistant starch; tubers.

Practical Application: Pyrodextrinization of cassava and sweet potato starch.

1 Introduction

Cassava (*M. esculenta*) and sweet potato (*I. batatas*) are tubers with an important production and distribution worldwide. Both are considered functional foods because they are a source of dietary fiber, vitamin C, thiamin, riboflavin, iron, magnesium, and phosphorus (Zhu, 2015; Kim et al., 2020). Furthermore, *M esculenta* and *I. batatas* can complete with corn which is the main source of starch worldwide due to their competitive production costs and both are currently considered as alternative sources of starch for the food industry (Toraya-Avilés et al., 2017; Akintayo et al., 2019). Starch is found in green leaves, seeds, cereals, and tubers and is the main source of energy in the human diet. The starch present in cassava and sweet potato ranges from 17 – 25 and 14.6 – 25%, respectively (Magallanes-Cruz et al., 2017; Kim et al., 2020). The use of native starch in the food industry is common, however it has limited functional properties, which is why it is modified (Ramos-García et al., 2018). Native starch (NS) can be subjected to physical, chemical, or enzymatic processes, producing the rupture or change in its molecular composition to improve its functional and physicochemical properties and enhance its consistency, viscosity and/or stability in the product. Such is the case of pyrodextrinization, in which bonds α 1 → 2, 1 → 3 and 1 → 6 are formed with a simultaneous reduction of a α 1 → 4 bonds, obtaining pyrodextrins with the ability to be resistant (RS) to digestive enzymes (Lovera et al., 2020). RS is not digested in the small intestine and is not absorbed; it reaches the colon and is fermented by bacteria in the microbiota. This promotes the production of short chain fatty acids (SCFA) that are taken up and used by L cells in the colon. Nonetheless, predicting the functionality of starch and explaining how it might interact with other food ingredients by analyzing its modifications and structures is a challenge. Therefore, the objective of this study was to evaluate the morphological and physicochemical changes of the native starch of *M. esculenta* and *I. batatas* after pyrodextrinization, including the production of RS and SDS.

2 Materials and methods

2.1 Raw materials and chemicals

The tubers *M. esculenta* and *I. batata* were purchased in a packing plant located at Villahermosa in the state of Tabasco, Mexico, and 30 kg of raw material for each fruit was obtained. All chemicals used for laboratory analyses were reagent grade (JT Baker, Phillipsburhg, NJ) and Megazyme (K-DSTRS 08/19; Megazyme © International Ireland 2008).

2.2 Starch isolation

The tubers were peeled and cut into 3 cm slices and each slice was further cut into four pieces, which were rinsed immediately in sodium bisulfite solution (0.25 g/l) in a 2:1 (v/w) proportion. Fruits were pureed in a blender (International LI-17) for 4 min and washed three times consecutively in water with 0.3% citric acid, using twice the volume of water than the cassava and sweet potato weight, and then it was sieved (100 mesh). The fiber retained on the sieve was removed, and the filtrate was kept in refrigeration (Asber ARR-17-1G-BL). The sediment was separated by decantation after 24 h. Starch was dried in an air furnace at atmospheric pressure for 24 h at 50 °C (Binder 23 ED). Starch was collected, ground (Krups GX410011), sieved (100 mesh) and stored in plastic bottles with hermetic lid closures (Toraya-Avilés et al., 2017).

2.3 Pyrodextrinization of starch

A 2^3 factorial design with four replicates of the central treatment was used. Factors were starch/acid (HCl 2.2 M) ratio (80:1 and 160:1 w/v); temperature (90 and 110 °C); and reaction time (1 and 3 h). The procedure (Toraya-Avilés et al., 2017) included 15 g of NS (dry basis; 12% moisture), which was placed in a 20 mL petri dish; HCl was added based on the ratio established for each treatment. The acid was allowed to react for 16 h. The Petri dishes were placed in a convection oven at the temperature and time corresponding to the treatment conditions. Pyrodextrinized starches were sieved (80 mesh). The RS and SDS yields (08/19 Megazyme) were determined. The response variable to evaluate the experiment was the RS yield.

2.4 Measurement of resistant and slowly digestible starch

Samples were incubated with pancreatic α-amylase and amyloglucosidase for 4 h at 37 °C in a stirred bath. Slowly digestible starch was recovered after 120 min and dissolved in acetate buffer; RS was recovered after 240 min and dissolved in 95% ethanol to stop the enzymatic reaction. Starch was quantitatively hydrolyzed to glucose by enzymatic action of amyloglucosidase and D-glucose was quantified with glucose oxidase/peroxidase reagent (Megazyme International Ireland), which represents the amount of RS present in the sample according to the Association of Official Analytical Chemists (AOAC) and the American Association of Cereal Chemists (AACC) internationally approved and validated methods (2002.02) and (32-40.01), respectively. The SDS content is represented in the following formula (Equation 1) (g/100 g sample):

$$SDS\,\% = \Delta A \, x \, F \, x \, EV \, / \, W \, x \, 0.0189 \tag{1}$$

RS content is represented as follows formula (Equation 2) (g/100 g sample):

$$RS\,\% = \Delta A \, x \, F \, x \, EV \, / \, W \, x \, FV \, x \, 0.000225 \tag{2}$$

Where:

ΔA = absorbance (reaction) read against the reagent blank after 20 min (RDS); after 120 min-20 min (SDS); after 240 min Total Digestible Starch (TDS).

F = conversion from absorbance to ug (the absorbance obtained for 100 ug of D-glucose in the GOPOD reaction is determined) [F = 100 (ug of D-glucose) divided by the GOPOD absorbance for this 100 ug of D-glucose]

EV = extraction vol (mL)

W = "as is" weight of sample analyzed in g; i.e. ~ 0.50 g or ~ 1.0 g.

FV/0.1 = 0.1 mL aliquots taken from final volume (FV; either 100 mL or 10.3 mL) for determination of glucose using GOPOD reagent

2.5 Scanning electron microscopy

Scanning electron microscopy was performed using a JEOL electronic microscope model JSM-7610F (FESEM, USA) with 1 nm resolution, 500 X magnification, micrograph of 10.3 mm, voltage accelerator of 5 kV, and probe current of up to 200 nA. Samples were placed on carbon conductive paper and metalating with a gold-platinum alloy for 1 min with the aid of a Quorum rotary coater model Q150R ES. Changes in size, shape, and granular structure resulting from treatments were recorded (Ottenhof & Farhat, 2004).

2.6 X-ray diffraction

X-ray diffraction was obtained with a diffractometer (Bruker D8-Advance, U.S.A.) using CuKα radiation (λ = 1.5418 Å) at 40 kV and 30 mA with an angular range (2-Theta) from 3° to 60° and a scan speed of 0.02° s⁻¹. The diffractometer was equipped with a copper source and operated at 40 kVg and 30 mA producing CuKα radiation with a wavelength of 1.54 Å. Data were collected in a range of 4° to 38° every 0.1° with a sweep rate of 60° s⁻¹. Baseline of the diffractogram was corrected in the sweep interval and the vector was normalized with the OPUS 3.0 program. The crystallinity was also determined (Nara & Komiya, 1983) and measured directly by plotting a curve connecting the peak baselines of the diffractograms. The area above the curve was taken as the crystalline portion, and the area under the curve was considered the amorphous portion. The area of the upper diffraction peak and the area of total diffraction over the diffraction angle were integrated into the EVA program version 4.1.1. (2015). Ratio of the area above the total area of diffraction was taken as the degree of crystallinity.

2.7 Functional characterization

Differential scanning calorimetry

The gelatinization temperature was determined using a DSC-6 (Perkin Elmer) with a heating rate of 10 °C min⁻¹ for NS and 5 °C for the chosen pyrodextrin; the heat flow ranged from 30 to 120 °C. The initial temperature (T_i), peak temperature (T_p), final temperature (T_f), and ΔH were obtained from the resulting thermogram (Ruales & Nair, 1994).

2.8 Solubility and swelling power

In a previously tared centrifuge tube with 50 mL capacity, 40 mL of a 1% (w/v) starch (dry basis) solution was prepared. A magnetic stirrer was then introduced into the tube and placed in a constant

temperature water bath (25, 60, 70, 80, or 90 °C) and stirred continuously for 30 min. Afterwards, its contents were dried and centrifuged at 2121 *x g* for 15 min. The supernatant was decanted, and the swollen granules of starch were weighed. Ten mL of the supernatant were placed to dry to a constant weight in a crucible at 120 °C for 4 h. Samples were transferred to a desiccator and weighed (Sathe & Salunkhe, 1981). The solubility and swelling power were calculated by the following formulas (Equation 3 and 4):

$$\%\,Solubility = \left(Soluble\ starch\ weight\ x\ 400 \right) / \left(Sample\ weight\,(d.b) \right) \quad (3)$$

$$Swelling\ capacity = \left(\left(Sediment\ weight \right) / \left(Sample\ weight\,(d.b) \right) \right) x\,(100 - \%\,solubility) \quad (4)$$

2.9 Water absorption capacity

The procedure was performed as previously described, but after centrifugation the resulting gel was weighed (P_2). The water absorption capacity was calculated as the weight (g) of the gel per gram of dry sample (Anderson et al., 1970).

2.10 Statistical analysis

Data were analyzed using descriptive statistics by calculating parameters of central tendency and dispersion. Pyrodextrinization results were analyzed by analysis of variance at a significance level of $p < 0.05$. The Duncan test was applied to determine the differences between the means. A regression analysis was also performed (Statgraphics plus 5.1).

3 Results

3.1 Starch isolation

The amounts of NS obtained from *M. esculenta* and *I. batatas* were 11.34 and 8.03% respectively.

3.2 Pyrodextrinization of starch

Manihot esculenta

The pyrodextrines from *M. esculenta* show RS values in a range of 16.06 – 24.42% (Table 1). According to the analyzed data, the factors starch/acid (HCl) 80:1, temperature (110 °C) and one hour of reaction time were significant ($p < 0.05$) to obtain the highest amount of RS. The mathematical model proposed to explain the behavior of the RS percentage is a function of the starch-acid concentration (A), temperature (B) and reaction time (C); as well as the interactions of starch-acid concentration/time (AC) and temperature/reaction time (BC), which is represented in the following Equation 5:

$$RS\,(\%) = 21.1675 - 1.3675\,(A) - 0.665\,(B) - 2.66\,(C) + 0.0975$$
$$- 0.5975\,(AC) - 0.28\,(BC) \quad (5)$$

The highest values were obtained in treatments 1 and 2 ($p<0.05$) where the highest proportion of acid was used.

3.3 Ipomoea batatas

The content RS values found in *I. batatas* showed a range of 20.90% - 47.15% after the pyrodextrinization process (Table 2). According to analysis of variance results, the significant factors ($p<0.05$) for the highest RS production were time and concentration. The concentration/temperature and concentration/time interactions also showed statistical significance. The concentration was the main effect for the highest production of RS.

The mathematical model proposed to explain the RS percentage behavior as a function of the starch-acid concentration (A), and reaction time (C), and the interactions of starch-acid concentration and temperature (AB) is represented in the following Equation 6:

$$RS\,(\%) = 40.175 - 2 - 38125\,(A) + 1.27875\,(B)$$
$$- 4.01875\,(C) + 3.16875\,(AB) - 2.21275\,(BC) - 0.10375 \quad (6)$$

The highest RS values were observed in treatments 3, 5 and 10 ($p < 0.05$), where the lowest proportion of acid was used.

Table 1. Resistant starch content and slowly digestible starch of *M. esculenta* native starch and pyrodextrine (d.m.).

Treatment	Starch/acid (HCl)	Temperature (°C)	Reaction time (h)	RS (%)	SDS (%)
1	80 a 1	90	1	24.12[a]	34.30[ab]
2	80 a 1	110	1	24.42[a]	33.60[ab]
3	160 a 1	90	1	23.64[a]	35.10[b]
4	160 a 1	110	1	21.81[b]	31.84[ab]
5	80 a 1	90	3	21.82[b]	38.25[bc]
6	80 a 1	110	3	18.46[c]	26.35[a]
7	160 a 1	90	3	16.43[d]	32.51[ab]
8	160 a 1	110	3	16.02[d]	44.56[c]
9	120 a 1	100	2	21.02[be]	36.28[b]
10	120 a 1	100	2	21.52[be]	37.41[b]
11	120 a 1	100	2	21.50[be]	37.70[b]
12	120 a 1	100	2	22.03[be]	34.40[b]
Native				14.52	51.12

RS: resistant starch; SDS: slowly digestible starch. [a-e] Different letter superscripts in the same column indicate a significant ($p<0.05$) difference.

3.4 Choice of the best pyrodextrinization treatments

The selection of the optimal pyrodextrinization treatment for both tubers was based on the observed variance data for the response variable RS. For *M. esculenta,* treatment 2 was selected and the conditions were high starch/acid (HCl 80:1) ratio, highest temperature (110 °C) and minimum reaction time (1 h). For *I. batatas,* treatment 5 was selected and the conditions were high starch/acid (HCl 80:1) ratio, lowest temperature (90 °C) and highest reaction time (3 h).

3.5 Determination of resistant and slowly digestible starch

The RS in NS of *M. esculenta* was 14.52% and 51.12% of SDS; after the pyrodextrinization process, the RS increased 10% (24.42%) and the SDS was 26.35%; these values show that as resistance increased, digestible starch decreased, and SDS was favorably preserved.

In the case of *I. batatas* in NS, 37.78% of RS and 16.7% of SDS were obtained. After the pyrodextrinization process, RS increased 10% (47.15%) and the SDS value was 26.71%.

3.6 Scanning electron microscopy

Figure 1a) shows the micrographs of NS granules from *M. esculenta* as spherical, oval, and truncated shapes with a diameter size of 4.69 μm to 17.2 μm. The pyrodextrin granules presented spherical, oval and some polygonal shapes with a diameter size of 16.1 μm to 20.8 μm (Figure 1b).

In Figure 2, the micrographs of *I. batatas* are shown; the NS granules (Figure 2a) were spherical, oval, and bell-shaped with a size of 5.34 μm to 24.1 μm; the pyrodextrin granules kept the same shapes, plus some polygonal granules with diameter values from 5.20 μm to 24.2 μm (Figure 2b).

The granules of both tubers were resistant to the acid treatment of pyrodextrinization, so there was no granular loss, which translates into the proportion of RS obtained for both sources.

3.7 X-ray diffraction

In Figure 3, the X-ray diffraction pattern of *M. esculenta* in its native form and in the pyrodextrin, was type C (mixture of pattern type A and B), presenting diffraction peaks at angles 5.6°, 10°, 15°,

Table 2. Resistant starch content and slowly digestible starch of *I. batatas* native starch and pyrodextrine (d.m.).

Treatment	Starch/acid (HCl)	Temperature	Reaction time	RS	SDS
		(°C)	(h)	(%)	(%)
1	80 a 1	90	1	39.83[bc]	20.33[bc]
2	80 a 1	110	1	43.88[c]	25.77[cd]
3	160 a 1	90	1	46.98[c]	17.83[b]
4	160 a 1	110	1	42.26[c]	5.43[a]
5	80 a 1	90	3	47.15[d]	21.49[bcd]
6	80 a 1	110	3	20.9[a]	21.26[bcd]
7	160 a 1	90	3	32.44[b]	26.71[e]
8	160 a 1	110	3	40.31[bc]	25.17[cd]
9	120 a 1	100	2	42.3[c]	17.06[b]
10	120 a 1	100	2	44.74[c]	19.68[b]
11	120 a 1	100	2	41.08[c]	19.27[b]
12	120 a 1	100	2	40.23[c]	17.32[b]
Native				37.78	16.7

RS: resistant starch; SDS: slowly digestible starch. [a-e] Different letter superscripts in the same column indicate a significant ($p < 0.05$) difference.
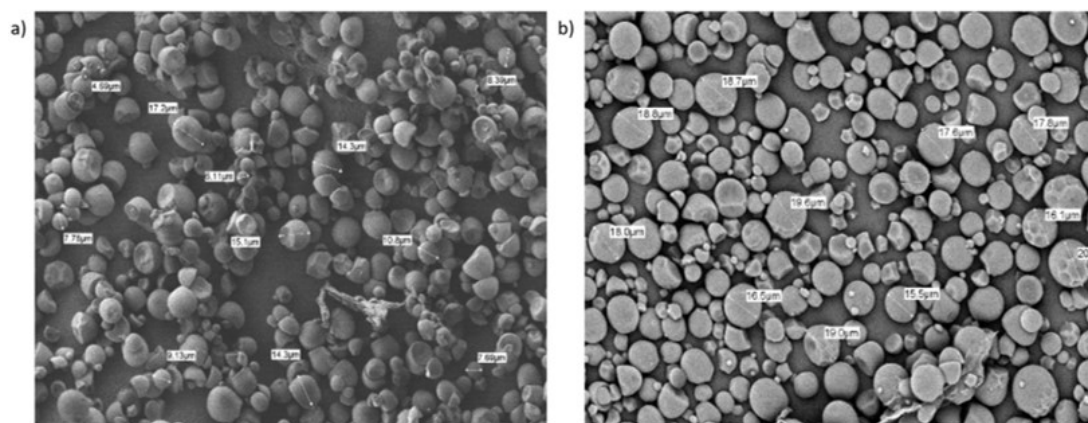
Figure 1. Micrograph of *M. esculenta* (a) native starch and (b) pyrodextrin.
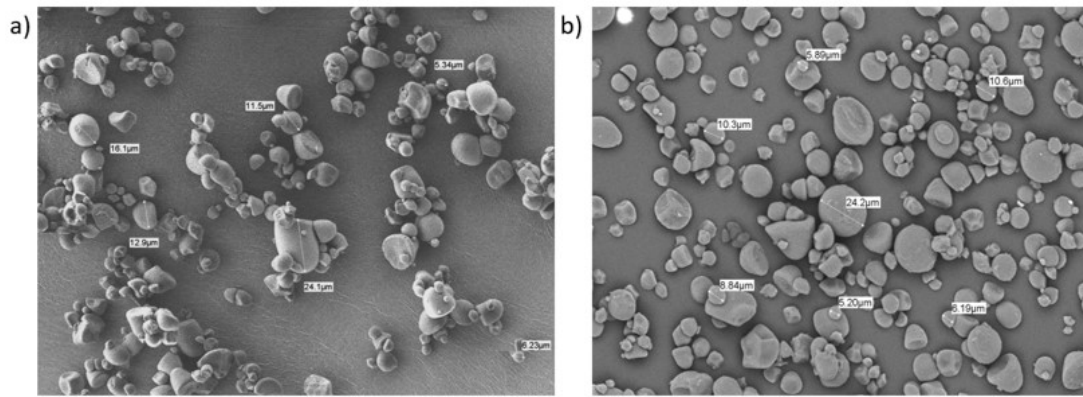
Figure 2. Micrograph of *I. batatas* (a) native starch and (b) pyrodextrin.

17°, 18° and 23°. The percentage of crystallinity of NS was 41.5%, decreasing to 35.4% in the pyrodextrin. Similarly, both RS and pyrodextrin from *I. batatas* presented a type C pattern (Figure 4) with diffraction peaks at angles 5.6°, 10°, 11.5°, 15°, 17°, 18°, 20°, 23° and 26.5°. The crystallinity observed in RS was 45.3% and in pyrodextrin 36.3%. A decrease in the crystallinity of both sources was observed after the modification, which could imply a morphological change caused by pyrodextrinization; the X-ray diffraction pattern indicates that the internal structure of the native granule was not destroyed or modified after the pyrodextrinization process.

3.8 Functional characterization

Differential scanning calorimetry

Figure 5 shows that the NS of *M. esculenta* has a ΔH of 1.3289 J/g and a gelatinization temperature of 64.56 °C (peak). In the pyrodextrin, the ΔH decreased slightly (0.9689 J/g) and the gelatinization temperature was 65.07 °C (peak).

Figure 6 shows that the NS of *I. batatas* has a ΔH de 9.6960 J/g and a temperature of 74.60 °C (peak); in the pyrodextrin, a ΔH of 2.6970 J/g and a gelatinization temperature of 76.16 °C (peak) were observed. Starch gelatinization evaluates the quality and perfection of the crystal in the internal structure of the granule. In this context, the loss of ΔH would demonstrate the loss of granular structure, however, although it decreased in both sources, the granular structure was still present, which corroborates that pyrodextrinization weakened the granule, but did not destroy the granular structure, which is consistent with the fact that resistance to digestion was not higher.

3.9 Solubility

The NS of *M. esculenta* showed a maximum solubility value of 11.97%, nevertheless, pyrodextrin showed a value of 12.76%; both values were obtained at 70 °C (Figure 7a). Conversely, the NS of *I. batatas* displayed a solubility of 6.07% at 70 °C, and its pyrodextrin reached the maximum solubility (15.12%) at the same temperature. The fact that the pyrodextrins present a higher solubility content corroborates the results obtained in the different morphological evaluation tests considering the effect on the granule after the chemical treatment is demonstrated, however, as 100% increase in solubility was not reached, the granular structure persists.
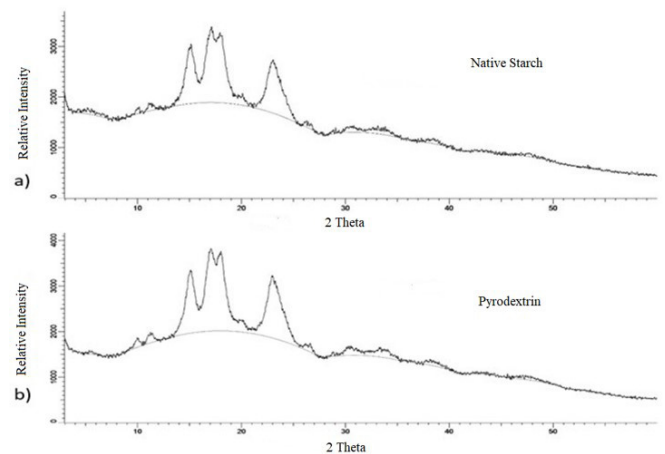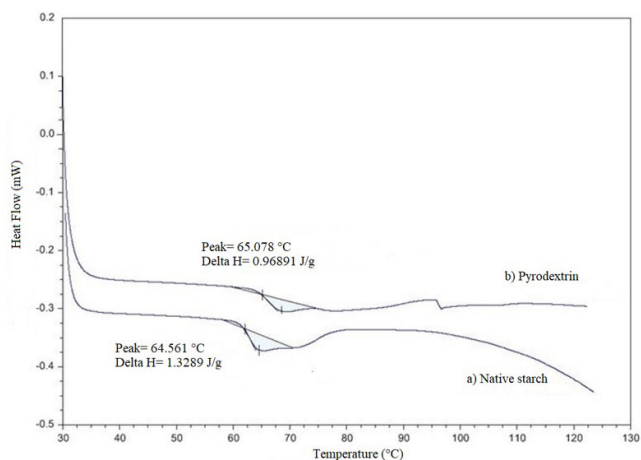

Figure 3. X-ray diffraction pattern of *M. esculenta* native starch and pyrodextrin.
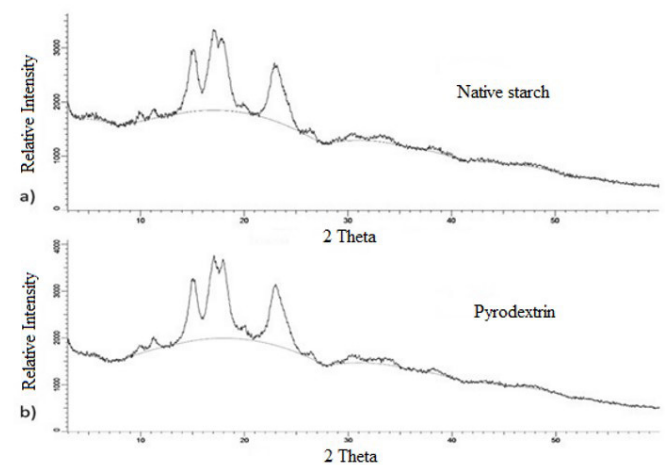

Figure 4. X-ray diffraction pattern of *I. batatas* native starch and pyrodextrin.

3.10 Swelling power

Figure 7b shows the maximum value of the swelling power of NS from *M. esculenta* at 70 °C with 14.98 g; however, its pyrodextrin occurs at 85 °C with 22.08 g. For the NS of *I. batatas*,

Figure 5. Differential scanning calorimetry thermogram of *M. esculenta* (a) native starch and (b) pyrodextrin.
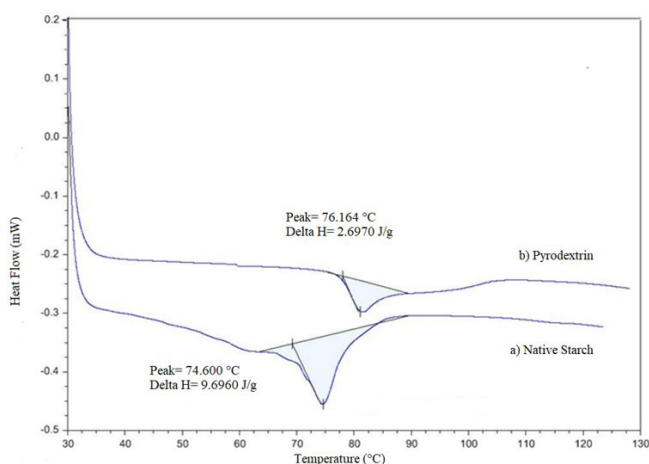
Figure 6. Differential scanning calorimetry thermogram of *I. batatas:* (a) native starch and (b) pyrodextrin.

Figure 7. Functional properties of *M. esculenta* native starch (NY), pyrodextrin of *M. esculenta* (PY), *I. batatas* native starch (NC) and pyrodextrin of *I. batatas* (PC): (a) solubility, (b) swelling power, and (c) water absorption capacity.
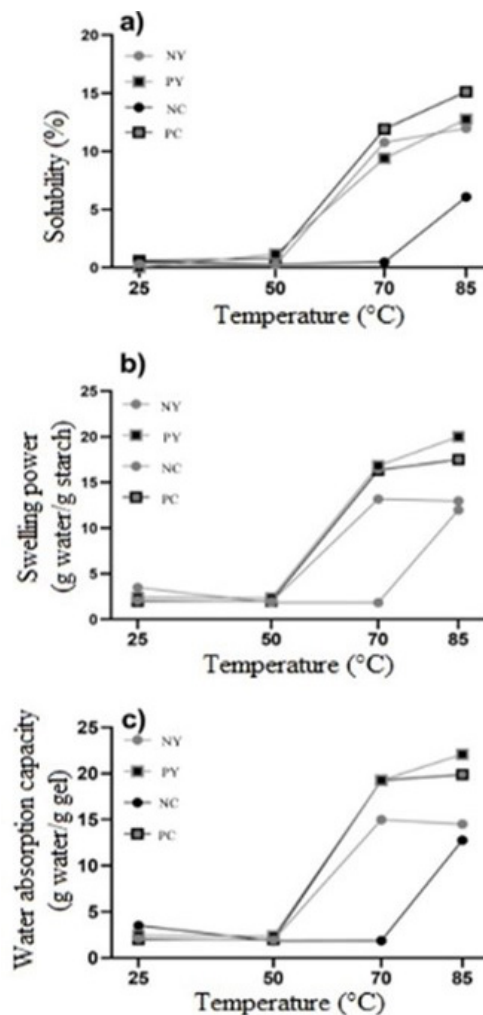
a maximum value of 12.76 g at 85 °C was observed and for its pyrodextrin it was 19.89 g at the same temperature. Both the swelling power and the water absorption capacity are closely linked. The increase in swelling power agrees with the resistance of the granules to total acid hydrolysis in pyrodextrinization, since it was possible to produce gels, which are more deformable than the gels obtained from granules with less swelling power.

3.11 Water absorption capacity

Figure 7c shows the maximum water absorption capacity of the NS from *M. esculenta,* which occurs at 85 °C with 13.18 g, and at the same temperature its pyrodextrin (20 g). In the case of NS from *I. batatas*, this functional property increases its maximum value at 85 °C with 11.98 g, and its pyrodextrine with 17.52 g.

4 Discussion

Guan et al. (2021) has shown that dietary fibers such as RS and SDS cannot be digested in the small intestine but are fermented in the colon. The intake of these dietary fibers has beneficial effects on the physiological state, such as the reduction of energy density of the diet, weight loss, decrease in blood glucose and insulin and the increase of fat oxidation in both humans and animal models (Villarroel et al., 2018). According to Khaturia et al. (2019), since SR is not absorbed, but fermented by the microbiota, it generates gases, short-chain fatty acids (SCFA), and small amounts of organic acids and alcohols, thus favoring the intestinal microbiota. As a result, the RS and SDS that can be found in NS stand out, however, in this form they present certain functional limitations, which is why they are modified (Toraya-Avilés et al., 2017). Such is the case of pyrodextrinization, which by forming atypical bonds in starch, promises to be an option to increase RS content, as reported by Betancur Ancona et al. (2020) in banana pyrodextrin and by Toraya-Avilés et al. (2017) in pyrodextrinized cassava.

The tubers are rich in starch and are a potential source to extract NS. In this work, a yield of 11.34 and 8.03% were obtained from *M. esculenta* and *I. batatas* (respectively); these

values were similar to those reported by Atwijukire et al. (2019) and Jiang et al. (2019). Regarding the products obtained by the pyrodextrinization treatment, in the case of both tubers, the highest concentration of acid was used; for cassava the shortest reaction time and the highest temperature were used, on the contrary, for the sweet potato it was the longest reaction time and the lowest temperature. Toraya-Avilés et al. (2017) reports the optimal treatment to pyrodextrinize cassava, also using the shortest reaction time and the highest temperature, and unlike the present study, they used the lowest concentration of acid. Rahman et al. (2020) reports that different genotypes among the same species can cause variation in the amount of RS, and SDS, including the morphology and crystalline organization of the granule.

It is noteworthy to mention that after the pyrodextrinization treatment, a maximum increase of 10% in its proportion of SR was observed in the NS of both sources. This could be explained by the formation of atypical bonds produced by acid hydrolysis, which gives starches less digestibility in the human gastrointestinal tract, but provides starch prebiotic properties (Bai & Shi, 2016). According to Zhang et al. (2020), there is the possibility of an increased number of α-1,6 glycosidic bonds, thus increasing resistance to digestion.

By means of the micrographs of the pyrodextrinized starch, granule ruptures were observed, as well as smaller granules of both *M. esculenta* and *I. batatas* caused by the effect of the treatment. However, resistant granules that preserved their spherical and oval shape were also observed. This coincides with findings by Wang et al. (2020) in pyrodextrins from *I. batatas*, where no apparent changes were observed after modification. This shows that the modification treatment applied to the NS was not enough to destroy the granule, and in this way the repolymerization with atypical bonds was carried out to observe an increase in the RS.

The same behavior could also be corroborated by evaluating the X-ray diffraction pattern, since for both sources, NS and pyrodextrinized starch, it was type C; this agrees with the findings reported by Lian et al. (2017) in tubers. The X-ray diffraction pattern type B is characteristic in sources with higher RS content according to Miao et al. (2015). Although the crystallinity of both pyrodextrins decreased slightly, it was enough to present an internal loss of the crystalline structure, reflecting fewer compact structures, due to the types of rhombic and hexagonal crystals present in its crystal structure (Cornejo-Ramírez et al., 2018). Regarding the functional properties evaluated, Cornejo-Ramírez et al. (2018) mention observing few changes in the gelatinization temperatures, as well as in the ΔH value after a modification treatment, which reflect that the double helices of the starch structure did not undergo important changes in the crystalline region. This result is consistent with the minor damage caused to the granule in the pyrodextrinization process and possibly the low formation of atypical bonds. In addition, due to the gelatinization temperatures observed in both sources, it is not feasible to include these ingredients in products subjected to high temperatures, however, they can be used in products that do not require high temperatures (candies, custards, puddings, beverages), thus contributing to the preservation of RS content while obtaining products in the food industry with benefits to human health.

5 Conclusions

Pyrodextrins with a 10% increase in RS were obtained for both cassava and sweet potato. The optimal pyrodextrinization conditions were the highest concentration of acid in both sources; for cassava, the shortest reaction time and the highest temperature were used; and for sweet potato it was the longest reaction time and the lowest temperature. The morphology of pyrodextrins was not completely affected after treatment, so it was possible that the formation of atypical bonds could not be carried out in its entirety to observe a greater increase in RS.

Acknowledgements

References

Akintayo, O. A., Obadu, J. M., Karim, O. R., Balogun, M. A., Kolawole, F. L., & Oyeyinka, S. A. (2019). Effect of replacement of cassava starch with sweet potato starch on the functional, pasting and sensory properties of tapioca grits. *LWT*, 111, 513-519. http://dx.doi.org/10.1016/j.lwt.2019.05.022.

Anderson, R., Conway, H., & Peplinski, A. J. (1970). Gelatinization of corn grits by roll cooking, extrusion cooking and steaming. *Stärke*, 22(4), 130-135. http://dx.doi.org/10.1002/star.19700220408.

Atwijukire, E., Hawumba, J. F., Baguma, Y., Wembabazi, E., Esuma, W., Kawuki, R. S., & Nuwamanya, E. (2019). Starch quality traits of improved provitamin A cassava (Manihot esculenta Crantz). *Heliyon*, 5(2), e01215. http://dx.doi.org/10.1016/j.heliyon.2019.e01215. PMid:30788444.

Bai, Y., & Shi, Y. C. (2016). Chemical structures in pyrodextrin determined by nuclear magnetic resonance spectroscopy. *Carbohydrate Polymers*, 151, 426-433. http://dx.doi.org/10.1016/j.carbpol.2016.05.058. PMid:27474585.

Betancur Ancona, D., Chel-Guerrero, L., Castellanos Ruelas, A. F., Sandoval-Peraza, V. M., Colin-Flores, R. F., Ble-Castillo, J. L., Juárez-Rojop, I. E., Acevedo-Fernández, J. J., Quintana-Owen, P., & Olvera Hernández, V. (2020). Efecto anticancerígeno del almidón modificado de banano (Musa cavendish AAA) en ratas con 1, 2-dimetilhidrazina. *Nutrición Hospitalaria*, 37(1), 147-154. PMid:31793323.

Cornejo-Ramírez, Y. I., Martínez-Cruz, O., Del Toro-Sánchez, C. L., Wong-Corral, F. J., Borboa-Flores, J., & Cinco-Moroyoqui, F. J. (2018). The structural characteristics of starches and their functional properties. *CYTA: Journal of Food*, 16(1), 1003-1017. http://dx.doi.org/10.1080/19476337.2018.1518343.

Guan, Z., Yu, E., & Feng, Q. (2021). Soluble dietary fiber, one of the most important nutrients for the gut microbiota. *Molecules (Basel, Switzerland)*, 26(22), 6802. http://dx.doi.org/10.3390/molecules26226802. PMid:34833893.

Jiang, Q., Liang, S., Zeng, Y., Lin, W., Ding, F., Li, Z., Cao, M., Li, Y., Ma, M., & Wu, Z. (2019). Morphology, structure and in vitro digestibility of starches isolated from Ipomoea batatas (L.) Lam. by alkali and ethanol methods. *International Journal of Biological Macromolecules*, 125, 1147-1155. http://dx.doi.org/10.1016/j.ijbiomac.2018.12.172. PMid:30578904.

Khaturia, D., Gautam, S., & Sharma, K. D. (2019). Utilization and health benefits of modified starch: a review. *International Journal of Current Agricultural Sciences*, 9, 347-358.

Kim, H., Woo, K. S., Lee, H.-U., Nam, S. S., Lee, B. W., Kim, M. Y., Lee, Y.-Y., Lee, J. Y., Kim, M. H., & Lee, B. (2020). Physicochemical characteristics of starch in sweet potato cultivars grown in Korea. *Preventive Nutrition and Food Science*, 25(2), 212-218. http://dx.doi.org/10.3746/pnf.2020.25.2.212. PMid:32676473.

Lian, X., Cheng, K., Wang, D., Zhu, W., & Wang, X. (2017). Analysis of crystals of retrograded starch with sharp X-ray diffraction peaks made by recrystallization of amylose and amylopectin. *International Journal of Food Properties*, 20(3), 3224-3236. http://dx.doi.org/10.1080/10942912.2017.1362433.

Lovera, M., Castro, G. M. C., Pires, N. R., Bastos, M. S. R., Holanda-Araújo, M. L., Laurentin, A., Moreira, R. A., & Oliveira, H. D. (2020). Pyrodextrinization of yam (Dioscorea sp.) starch isolated from tubers grown in Brazil and physicochemical characterization of yellow pyrodextrins. *Carbohydrate Polymers*, 242, 116382. http://dx.doi.org/10.1016/j.carbpol.2020.116382. PMid:32564854.

Magallanes-Cruz, P. A., Flores-Silva, P. C., & Bello-Perez, L. A. (2017). Starch structure influences its digestibility: a review. *Journal of Food Science*, 82(9), 2016-2023. http://dx.doi.org/10.1111/1750-3841.13809. PMid:28753728.

Miao, M., Jiang, B., Cui, S., Tao Zhang, T., & Jin, Z. (2015). Slowly digestible starch: a review. *Food Science & Nutrition*, 55(12), 1642-1657. PMid:24915311.

Nara, S., & Komiya, T. (1983). Studies on the relationship between water-satured state and crystallinity by the diffraction method for moistened potato starch. *Stärke*, 35(12), 407-410. http://dx.doi.org/10.1002/star.19830351202.

Ottenhof, M.-A., & Farhat, I. A. (2004). The effect of gluten on the retrogradation of wheat starch. *Journal of Cereal Science*, 40(3), 269-274. http://dx.doi.org/10.1016/j.jcs.2004.07.002.

Rahman, N., Ajie, F. T., & Hartati, N. S. (2020). Variation of cassava genotypes based on physicochemical properties of starches and resistant starch content. In *IOP Conference Series: Earth and Environmental Science* (Vol. 439, pp. 012048). Bristol: IOP Publishing.

Ramos-García, M. L., Romero-Bastida, C., & Bautista-Baños, S. (2018). Modified starch: properties and uses as edible coatings for the preservation of fresh fruits and vegetables. *Revista Iberoamericana de Tecnología Postcosecha*, 19(1), 30-44.

Ruales, J., & Nair, B. M. (1994). Properties of starch and dietary fibre in raw and processed quinoa (Chenopodium quinoa, Willd) seeds. *Plant Foods for Human Nutrition (Dordrecht, Netherlands)*, 45(3), 223-246. http://dx.doi.org/10.1007/BF01094092. PMid:8052579.

Sathe, S., & Salunkhe, D. K. (1981). Isolation, partial characterization and modification of the great northern bean (Phaseolus vulgaris L.) starch. *Journal of Food ScienceVolume*, 46(2), 617-621. http://dx.doi.org/10.1111/j.1365-2621.1981.tb04924.x.

Toraya-Avilés, R., Segura-Campos, M., Chel-Guerrero, L., & Betancur-Ancona, D. (2017). Effects of pyroconversion and enzymatic hydrolysis on indigestible starch content and physicochemical properties of cassava (Manihot esculenta) starch. *Stärke*, 69(5-6), 1600267. http://dx.doi.org/10.1002/star.201600267.

Villarroel, P., Gómez, C., Vera, C., & Torres, J. (2018). Almidón resistente: características tecnológicas e intereses fisiológicos. *Revista Chilena de Nutrición*, 45(3), 271-278. http://dx.doi.org/10.4067/s0717-75182018000400271.

Wang, H., Yang, Q., Ferdinand, U., Gong, X., Qu, Y., Gao, W., Ivanistau, A., Feng, B., & Liu, M. (2020). Isolation and characterization of starch from light yellow, orange, and purple sweet potatoes. *International Journal of Biological Macromolecules*, 160, 660-668. http://dx.doi.org/10.1016/j.ijbiomac.2020.05.259. PMid:32497669.

Zhang, X., Leemhuis, H., & van der Maarel, M. J. (2020). Digestion kinetics of low, intermediate and highly branched maltodextrins produced from gelatinized starches with various microbial glycogen branching enzymes. *Carbohydrate Polymers*, 247, 116729. http://dx.doi.org/10.1016/j.carbpol.2020.116729. PMid:32829851.

Zhu, F. (2015). Composition, structure, physicochemical properties, and modifications of cassava starch. *Carbohydrate Polymers*, 122, 456-480. http://dx.doi.org/10.1016/j.carbpol.2014.10.063. PMid:25817690.